

## A PHOTOMETRIC ANALYSIS OF SEVENTEEN BINARY STARS USING SPECKLE IMAGING

JAMES W. DAVIDSON JR.<sup>1,6</sup>, BRIAN J. BAPTISTA<sup>2,6</sup>, ELLIOTT P. HORCH<sup>3,6,7,8</sup>, OTTO FRANZ<sup>4,6,7</sup>, AND WILLIAM F. VAN ALTENA<sup>5,6</sup>

<sup>1</sup> Department of Physics and Astronomy, The University of Toledo, 2801 West Bancroft Street, Toledo, OH 43606-3390, USA; [jdavid@physics.utoledo.edu](mailto:jdavid@physics.utoledo.edu)

<sup>2</sup> Department of Astronomy, Indiana University, 727 East 3rd Street, Bloomington, IN 47405-7105, USA; [bbapti@astro.indiana.edu](mailto:bbapti@astro.indiana.edu)

<sup>3</sup> Department of Physics, Southern Connecticut State University, 501 Crescent Street, New Haven, CT 06515, USA; [horche2@southernct.edu](mailto:horche2@southernct.edu)

<sup>4</sup> Lowell Observatory, 1400 West Mars Hill Road, Flagstaff, AZ 86001, USA; [Otto.Franz@lowell.edu](mailto:Otto.Franz@lowell.edu)

<sup>5</sup> Department of Astronomy, Yale University, P.O. Box 208101, New Haven, CT 06520, USA; [william.vanaltena@yale.edu](mailto:william.vanaltena@yale.edu)

Received 2008 February 11; accepted 2009 August 19; published 2009 September 30

### ABSTRACT

Magnitude differences obtained from speckle imaging are used in combination with other data in the literature to place the components of binary star systems on the H–R diagram. Isochrones are compared with the positions obtained, and a best-fit isochrone is determined for each system, yielding both masses of the components as well as an age range consistent with the system parameters. Seventeen systems are studied, 12 of which were observed with the 0.6 m Lowell-Tololo Telescope at Cerro Tololo Inter-American Observatory and six of which were observed with the WIYN 3.5 m Telescope (The WIYN Observatory is a joint facility of the University of Wisconsin-Madison, Indiana University, Yale University, and the National Optical Astronomy Observatories) at Kitt Peak. One system was observed from both sites. In comparing photometric masses to mass information from orbit determinations, we find that the photometric masses agree very well with the dynamical masses, and are generally more precise. For three systems, no dynamical masses exist at present, and therefore the photometrically determined values are the first mass estimates derived for these components.

*Key words:* binaries: visual – techniques: high angular resolution – techniques: interferometric – techniques: photometric

### 1. INTRODUCTION

Since its inception in the 1970s, speckle interferometry has been an important technique for determining high-quality orbits of visual binary stars. The outstanding astrometric precision of the technique in particular has made it possible to collect valuable data even from small-aperture telescopes, most notably the 0.66 m refractor at the U.S. Naval Observatory in Washington, DC; see Mason et al. (2007) and references therein. Our group has also done a substantial amount of small-aperture speckle interferometry, mainly in the Southern Hemisphere, from both the 0.76 m telescope at El Leoncito, Argentina (Horch et al. 1996, 2006b) and 0.60 m telescopes at Las Campanas and Cerro Tololo, Chile, e.g., Horch et al. (2006a) and references therein. We have also contributed a substantial number of measures from the WIYN 3.5 m Telescope, the most recent group of which is detailed in Horch et al. (2008).

Photometric information has traditionally been more difficult to obtain from speckle interferometry, though this situation has improved in recent years. For example, magnitude difference measures of subarcsecond binaries obtained with the RIT-Yale Tip-Tilt Speckle Imager (RYTSI) at the WIYN 3.5 m Telescope have an average precision of 0.10 mag per two-minute observation (Horch et al. 2008). RYTSI uses a large-format CCD detector as the image capture device, as detailed in Meyer et al. (2006). At smaller apertures, CCD-based speckle photometry has shown no significant systematic deviations from

space-based measures, however, measurement precision is poorer compared to larger-aperture work. In the observations described above at Las Campanas and Cerro Tololo (where a CCD was again used to image the speckle patterns), the uncertainty per two-minute observation is 0.15–0.18 mag for typical observing conditions. A color formed from two such observations in two different filters would of course be even more uncertain.

Nonetheless, with repeated observations of a binary using a small telescope, these uncertainties can in theory be brought down to the point where meaningful comparisons with stellar structure and evolution calculations can be made. In addition, when using a smaller telescope, the effects of atmospheric dispersion are less evident on individual speckles and therefore a wider filter can be used. For the Las Campanas and Cerro Tololo observations, Bessel *B*, *V*, and *R* filters were used. This has the advantage that the photometry obtained is already on a well-understood photometric system. On the other hand, at a larger aperture such as WIYN, narrow filters must be used to maintain good speckle contrast, and this necessarily presents an additional obstacle in interpreting the photometry; however, such observations have intrinsically better precision.

The primary goal of the study presented here is to demonstrate that the individual components of binary systems can be placed with precision on the H–R diagram using either small-aperture speckle photometry (where standard filters are used) or larger-aperture speckle photometry such as at WIYN (where non-standard filters are used, but can be calibrated onto a standard system). Theoretical isochrones can then be fit to the locations of the stars, yielding mass estimates of the components and a basic age estimate of the system, assuming the system is coeval. This allows for two types of further analysis. First, in cases where a high-quality orbit already exists, the mass information available further constrains the isochrone match, since only a small segment of the isochrone is a permissible match for each

<sup>6</sup> Visiting Astronomer, Kitt Peak National Observatory, National Optical Astronomy Observatory, which is operated by the Association of Universities for Research in Astronomy, Inc. (AURA) under cooperative agreement with the National Science Foundation.

<sup>7</sup> Visiting Astronomer, Cerro Tololo Inter-American Observatory, National Optical Astronomy Observatory, which is operated by the Association of Universities for Research in Astronomy, Inc. (AURA) under cooperative agreement with the National Science Foundation.

<sup>8</sup> Adjunct Astronomer, Lowell Observatory.

component. If sufficient precision can be brought to bear, this leads to direct tests of stellar structure and evolution models. Second, since many visual binaries have orbital periods that are tens or hundreds of years, this method of mass determination would be extremely useful in completing statistical studies of binaries in a relatively short period of time. In this way, mass could be correlated with other properties, such as spatial location relative to the Galactic disk and metallicity, to better understand any differences between distinct binary populations.

## 2. OBSERVATIONS AND ANALYSIS

In this paper, we present results from both the Lowell-Tololo 0.6 m Telescope at Cerro Tololo Inter-American Observatory (CTIO), and the WIYN 3.5 m Telescope at Kitt Peak National Observatory. In the case of the Lowell-Tololo observations, data from two runs were combined: 1999 October 5–18 and 2001 November 9–22. A Kodak KAF-4200 front-illuminated CCD was used to capture the speckle images on both occasions. The 1999 run includes only data taken in the  $V$  and  $R$  filters, while the 2001 run also incorporated the use of a  $B$  filter. All three filters were provided by Rochester Institute of Technology (RIT), where one of us (E.H.) was a faculty member at the time. Photometric results from these runs appear in Horch et al. (2001, 2006a). The filters were presumed to be Bessel filters in Horch et al. (2006a); however, subsequent comparisons of the transmission curves against those by Bessel (1990) showed differences, as seen in Figure 1.

WIYN photometric data come from the long program of speckle observations that our group has had there. Photometric results are found in Horch et al. (2004, 2008), and span the time frame of 1997 through 2006. During that interval, two different speckle systems were used, though usually with the same CCD that was used in the Lowell-Tololo observations. More information about the speckle optics used during 1997–2000 can be found in Horch et al. (1999), while from 2001–2006, the RYTSI speckle camera was used.

Although hundreds of binaries were observed at both telescopes, in our initial study, we sought to analyze systems that were well observed and had no major or recent indication of variability. For Lowell-Tololo data, we required at least three independent observations in each of the  $V$  and  $R$  filters. If the  $B$  filter data were also included, three observations were required here as well. For WIYN data, at least two observations were required in each of the three different filters. Because of the larger aperture, these data have greater precision, and so we judged it sufficient to reduce the number of observations in a given filter from three to two. Objects that survived these data cuts were then checked for variability in the General Catalog of Variable Stars (GCVS)<sup>9</sup> of Samus' et al. (2006). Most of our objects had no entry in that source, but in four cases, namely, STF 186, GLE 1, AC 4, and BU 178 (HIP 8998, 19917, 32677, and 113184, respectively), we retained the object even though it did have an entry in the GCVS. For these objects, the amplitude and type of the variation was either not given or sufficiently small for our purposes ( $<0.02$  mag). We then examined the data in the *Hipparcos* Catalog (ESA 1997) and the General Catalog of Photometric Data (GCPD)<sup>10</sup> of Mermilliod et al. (1997) and found no evidence of variability significant on the level of this study. All four of these objects were observed at the Lowell-Tololo Telescope. We also checked the reddening and extinction

toward each object using the NASA/IPAC dust map available online,<sup>11</sup> and found that, as expected due to the relatively small distances to our objects, no correction was needed at the level of our photometry.

Tables 1 and 2 contain the final object lists and input data used in this study for CTIO and WIYN data, respectively. In both cases, the table columns give (1) the Washington Double Star<sup>12</sup> (WDS) Catalog number for the system (Mason et al. 2001), which also gives the right ascension and declination of the object in J2000.0 coordinates; (2) the discoverer designation in the WDS for the system; (3) the *Hipparcos* Catalog number; (4) the filter used; (5) the number of observations of the system in that filter; (6) the Johnson  $V$  magnitude of the system; (7) the Johnson  $B - V$  color of the system; (8) the parallax of the system, as it appears in the *Hipparcos* Catalog; and (9) the log of the iron abundance compared to the solar value ( $[Fe/H]$ ), if known. In most cases, the system  $V$  magnitude and  $B - V$  color are the average of the Johnson UBV values appearing in the GCPD. The uncertainties given are the standard errors computed from the GCPD data. If no data were available for a particular star in the GCPD, then the values shown in the *Hipparcos* Catalog were used. Iron abundances are from the Geneva-Copenhagen Catalog (Nordström et al. 2004) unless otherwise stated.

### 2.1. Magnitude and Color Conversions

Since the RIT filters differ from Bessel filters, the Fernie (1983) transformation equations used in Horch et al. (2001) can be improved. In addition,  $B - V$  colors and apparent  $V$  magnitudes for the binaries are in the standard Johnson filter set (Johnson 1965), which also have slight differences with the Bessel standard filters. Similarly, for WIYN data, a system of transformation equations was needed to convert between the narrow instrumental filters and the Johnson system. The approach here has been a four-step process, which is described in further detail below, and is summarized as follows. (1) The Pickles spectral library (Pickles 1998) was used to develop the transformations to convert the system  $V$  magnitudes and  $B - V$  colors to instrumental values for the desired speckle filters. (2) The  $V$  and  $B - V$  values for each system were then converted to instrumental values using these results. (3) These were then used in combination with the speckle magnitude differences to obtain *component* magnitudes and colors in the speckle filters. (4) Finally, these values were converted back to the Johnson system. The final results in the Johnson system could then be used for isochrone fitting.

The Pickles spectral library (Pickles 1998), containing 131 sample spectra, was used to simulate magnitude measurements, along with the filter and atmospheric transmission curves and the quantum efficiency curve for the CCD. For a filter  $x$ , the stellar flux in that filter,  $f_x$ , is therefore expressed as

$$f_x = \int_0^\infty S A F_x Q d\lambda, \quad (1)$$

where  $S$  is the star's flux,  $A$  is the atmospheric transmission curve,  $F_x$  is the filter transmission curve, and  $Q$  is the quantum efficiency of the CCD. In addition, there are losses in the optical system, but these are assumed small enough to ignore in this study. From such a flux, a magnitude is then determined.

The filter transmission data for the Johnson UBV filters are available at the GCPD Web site. Magnitude values for stars in the

<sup>9</sup> <http://www.sai.msu.su/groups/cluster/gcvs/gcvs/>

<sup>10</sup> <http://obswww.unige.ch/gcpd/gcpd.html>

<sup>11</sup> <http://irsa.ipac.caltech.edu/applications/DUST/>

<sup>12</sup> <http://ad.usno.navy.mil/wds/>

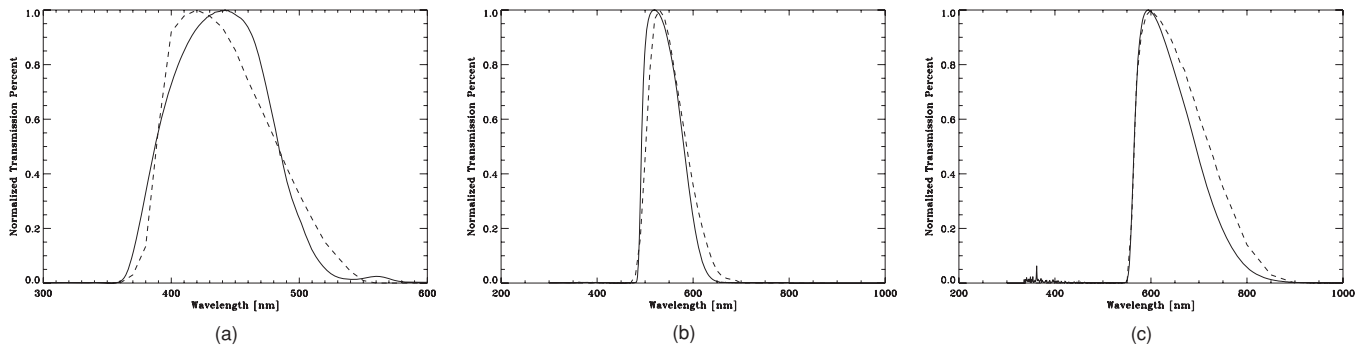


**Figure 1.** Normalized transmission curves of the RIT filters, solid lines, and the Bessel filters, dashed lines for (a) *B* filter, (b) *V* filter, and (c) *R* filter.

**Table 1**  
Speckle Magnitude Differences and Additional Input Parameters, CTIO Data

WDS ( $\alpha$ , $\delta$ J2000.0)	Discoverer Designation	HIP	Speckle Data			System Parameters																																																																																																																																																				
			Filter	No. of Obs.	$\Delta m$ (mag)	$V^a$ (mag)	$B - V^a$ (mag)	Parallax <sup>b</sup> (mas)	[Fe/H]																																																																																																																																																	
00373–2446	BU 395	2941	<i>V</i>	5	$0.25 \pm 0.14$	$5.570 \pm 0.005$	$0.722 \pm 0.008$	$64.38 \pm 1.40$	–0.12																																																																																																																																																	
			<i>R</i>	5	$0.33 \pm 0.19$					01243–0655	BU 1163	6564	<i>V</i>	6	$0.19 \pm 0.06$	$5.908 \pm 0.004$	$0.404 \pm 0.009$	$22.33 \pm 0.95$	–0.25	<i>R</i>	8	$0.27 \pm 0.08$	01361–2954	HJ 3447	7463	<i>V</i>	7	$1.05 \pm 0.06$	$5.685 \pm 0.005$	$0.335 \pm 0.005$	$16.13 \pm 0.97$	+0.01	<i>R</i>	5	$1.17 \pm 0.02$	01559 + 0151	STF 186	8998	<i>B</i>	3	$0.76 \pm 0.26$	$6.007 \pm 0.004$	$0.549 \pm 0.005$	$25.71 \pm 1.73$	–0.12	<i>V</i>	8	$0.56 \pm 0.09$	<i>R</i>	5	$0.56 \pm 0.04$	03124–4425	JC 8AB	14913	<i>B</i>	3	$0.59 \pm 0.06$	$5.920 \pm 0.010^b$	$0.440 \pm 0.042^b$	$22.83 \pm 0.78$	–0.08	<i>V</i>	6	$0.40 \pm 0.11$	<i>R</i>	6	$0.55 \pm 0.08$	04163–6057	GLE 1	19917	<i>V</i>	3	$0.44 \pm 0.38$	$6.360 \pm 0.006$	$0.073 \pm 0.007$	$08.41 \pm 0.53$	...	<i>R</i>	4	$0.27 \pm 0.21$	05079 + 0830	STT 98	23879	<i>V</i>	6	$1.18 \pm 0.06$	$5.331 \pm 0.004$	$0.333 \pm 0.004$	$16.84 \pm 1.32$	...	<i>R</i>	5	$1.04 \pm 0.06$	06490–1509	AC 4	32677	<i>B</i>	3	$1.82 \pm 0.06$	$5.390 \pm 0.006$	$-0.100 \pm 0.000$	$05.37 \pm 0.86$	...	<i>V</i>	6	$1.71 \pm 0.08$	<i>R</i>	4	$1.71 \pm 0.08$	20375+1436	BU 151AB	101769	<i>V</i>	8	$1.20 \pm 0.05$	$3.617 \pm 0.016$	$0.458 \pm 0.019$	$33.49 \pm 0.88$	–0.05 <sup>c</sup>	<i>R</i>	7	$1.14 \pm 0.06$	22300+0426	STF 2912	111062	<i>V</i>	6	$1.50 \pm 0.06$	$5.494 \pm 0.008$	$0.387 \pm 0.006$	$18.93 \pm 1.23$	+0.34 <sup>d</sup>	<i>R</i>	4	$1.35 \pm 0.07$	22552–0459	BU 178	113184	<i>V</i>	3	$1.76 \pm 0.10$	$5.715 \pm 0.005$	$0.880 \pm 0.000$	$11.13 \pm 0.95$	+0.09 <sup>e</sup>	<i>R</i>	5	$1.95 \pm 0.10$	23357–2729	SEE 492	116436	<i>V</i>	6	$1.70 \pm 0.04$
01243–0655	BU 1163	6564	<i>V</i>	6	$0.19 \pm 0.06$	$5.908 \pm 0.004$	$0.404 \pm 0.009$	$22.33 \pm 0.95$	–0.25																																																																																																																																																	
			<i>R</i>	8	$0.27 \pm 0.08$					01361–2954	HJ 3447	7463	<i>V</i>	7	$1.05 \pm 0.06$	$5.685 \pm 0.005$	$0.335 \pm 0.005$	$16.13 \pm 0.97$	+0.01	<i>R</i>	5	$1.17 \pm 0.02$	01559 + 0151	STF 186	8998	<i>B</i>	3	$0.76 \pm 0.26$	$6.007 \pm 0.004$	$0.549 \pm 0.005$	$25.71 \pm 1.73$	–0.12	<i>V</i>	8	$0.56 \pm 0.09$				<i>R</i>	5	$0.56 \pm 0.04$					03124–4425	JC 8AB	14913	<i>B</i>	3	$0.59 \pm 0.06$				$5.920 \pm 0.010^b$	$0.440 \pm 0.042^b$	$22.83 \pm 0.78$					–0.08	<i>V</i>	6	$0.40 \pm 0.11$	<i>R</i>	6	$0.55 \pm 0.08$	04163–6057	GLE 1	19917	<i>V</i>	3	$0.44 \pm 0.38$	$6.360 \pm 0.006$	$0.073 \pm 0.007$	$08.41 \pm 0.53$	...	<i>R</i>	4	$0.27 \pm 0.21$	05079 + 0830	STT 98	23879	<i>V</i>	6	$1.18 \pm 0.06$	$5.331 \pm 0.004$	$0.333 \pm 0.004$	$16.84 \pm 1.32$	...	<i>R</i>	5				$1.04 \pm 0.06$	06490–1509	AC 4					32677	<i>B</i>	3	$1.82 \pm 0.06$	$5.390 \pm 0.006$	$-0.100 \pm 0.000$	$05.37 \pm 0.86$	...	<i>V</i>	6	$1.71 \pm 0.08$	<i>R</i>	4	$1.71 \pm 0.08$	20375+1436	BU 151AB	101769	<i>V</i>	8	$1.20 \pm 0.05$	$3.617 \pm 0.016$	$0.458 \pm 0.019$	$33.49 \pm 0.88$	–0.05 <sup>c</sup>	<i>R</i>	7	$1.14 \pm 0.06$	22300+0426	STF 2912	111062	<i>V</i>	6	$1.50 \pm 0.06$	$5.494 \pm 0.008$	$0.387 \pm 0.006$	$18.93 \pm 1.23$	+0.34 <sup>d</sup>	<i>R</i>	4	$1.35 \pm 0.07$	22552–0459	BU 178	113184	<i>V</i>	3	$1.76 \pm 0.10$	$5.715 \pm 0.005$	$0.880 \pm 0.000$	$11.13 \pm 0.95$	+0.09 <sup>e</sup>	<i>R</i>
01361–2954	HJ 3447	7463	<i>V</i>	7	$1.05 \pm 0.06$	$5.685 \pm 0.005$	$0.335 \pm 0.005$	$16.13 \pm 0.97$	+0.01																																																																																																																																																	
			<i>R</i>	5	$1.17 \pm 0.02$					01559 + 0151	STF 186	8998	<i>B</i>	3	$0.76 \pm 0.26$	$6.007 \pm 0.004$	$0.549 \pm 0.005$	$25.71 \pm 1.73$	–0.12	<i>V</i>	8	$0.56 \pm 0.09$				<i>R</i>	5	$0.56 \pm 0.04$					03124–4425	JC 8AB	14913	<i>B</i>	3	$0.59 \pm 0.06$	$5.920 \pm 0.010^b$	$0.440 \pm 0.042^b$	$22.83 \pm 0.78$	–0.08	<i>V</i>	6	$0.40 \pm 0.11$				<i>R</i>	6	$0.55 \pm 0.08$	04163–6057	GLE 1	19917				<i>V</i>	3	$0.44 \pm 0.38$	$6.360 \pm 0.006$		$0.073 \pm 0.007$	$08.41 \pm 0.53$	...	<i>R</i>	4	$0.27 \pm 0.21$	05079 + 0830	STT 98	23879	<i>V</i>	6	$1.18 \pm 0.06$	$5.331 \pm 0.004$	$0.333 \pm 0.004$	$16.84 \pm 1.32$	...	<i>R</i>	5	$1.04 \pm 0.06$	06490–1509	AC 4	32677	<i>B</i>	3	$1.82 \pm 0.06$	$5.390 \pm 0.006$	$-0.100 \pm 0.000$	$05.37 \pm 0.86$	...	<i>V</i>	6	$1.71 \pm 0.08$	<i>R</i>	4	$1.71 \pm 0.08$			20375+1436	BU 151AB	101769	<i>V</i>		8	$1.20 \pm 0.05$	$3.617 \pm 0.016$					$0.458 \pm 0.019$	$33.49 \pm 0.88$	–0.05 <sup>c</sup>	<i>R</i>	7	$1.14 \pm 0.06$	22300+0426	STF 2912	111062	<i>V</i>	6	$1.50 \pm 0.06$	$5.494 \pm 0.008$	$0.387 \pm 0.006$	$18.93 \pm 1.23$	+0.34 <sup>d</sup>	<i>R</i>	4	$1.35 \pm 0.07$	22552–0459	BU 178	113184	<i>V</i>	3	$1.76 \pm 0.10$	$5.715 \pm 0.005$	$0.880 \pm 0.000$	$11.13 \pm 0.95$	+0.09 <sup>e</sup>	<i>R</i>	5	$1.95 \pm 0.10$	23357–2729	SEE 492	116436	<i>V</i>	6	$1.70 \pm 0.04$	$6.650 \pm 0.010$	$0.560 \pm 0.000$	$25.96 \pm 1.11$	–0.10	<i>R</i>
01559 + 0151	STF 186	8998	<i>B</i>	3	$0.76 \pm 0.26$	$6.007 \pm 0.004$	$0.549 \pm 0.005$	$25.71 \pm 1.73$	–0.12																																																																																																																																																	
			<i>V</i>	8	$0.56 \pm 0.09$																																																																																																																																																					
			<i>R</i>	5	$0.56 \pm 0.04$																																																																																																																																																					
03124–4425	JC 8AB	14913	<i>B</i>	3	$0.59 \pm 0.06$	$5.920 \pm 0.010^b$	$0.440 \pm 0.042^b$	$22.83 \pm 0.78$	–0.08																																																																																																																																																	
			<i>V</i>	6	$0.40 \pm 0.11$																																																																																																																																																					
			<i>R</i>	6	$0.55 \pm 0.08$																																																																																																																																																					
04163–6057	GLE 1	19917	<i>V</i>	3	$0.44 \pm 0.38$	$6.360 \pm 0.006$	$0.073 \pm 0.007$	$08.41 \pm 0.53$	...																																																																																																																																																	
			<i>R</i>	4	$0.27 \pm 0.21$																																																																																																																																																					
05079 + 0830	STT 98	23879	<i>V</i>	6	$1.18 \pm 0.06$	$5.331 \pm 0.004$	$0.333 \pm 0.004$	$16.84 \pm 1.32$	...																																																																																																																																																	
			<i>R</i>	5	$1.04 \pm 0.06$																																																																																																																																																					
06490–1509	AC 4	32677	<i>B</i>	3	$1.82 \pm 0.06$	$5.390 \pm 0.006$	$-0.100 \pm 0.000$	$05.37 \pm 0.86$	...																																																																																																																																																	
			<i>V</i>	6	$1.71 \pm 0.08$																																																																																																																																																					
			<i>R</i>	4	$1.71 \pm 0.08$																																																																																																																																																					
20375+1436	BU 151AB	101769	<i>V</i>	8	$1.20 \pm 0.05$	$3.617 \pm 0.016$	$0.458 \pm 0.019$	$33.49 \pm 0.88$	–0.05 <sup>c</sup>																																																																																																																																																	
			<i>R</i>	7	$1.14 \pm 0.06$																																																																																																																																																					
22300+0426	STF 2912	111062	<i>V</i>	6	$1.50 \pm 0.06$	$5.494 \pm 0.008$	$0.387 \pm 0.006$	$18.93 \pm 1.23$	+0.34 <sup>d</sup>																																																																																																																																																	
			<i>R</i>	4	$1.35 \pm 0.07$																																																																																																																																																					
22552–0459	BU 178	113184	<i>V</i>	3	$1.76 \pm 0.10$	$5.715 \pm 0.005$	$0.880 \pm 0.000$	$11.13 \pm 0.95$	+0.09 <sup>e</sup>																																																																																																																																																	
			<i>R</i>	5	$1.95 \pm 0.10$																																																																																																																																																					
23357–2729	SEE 492	116436	<i>V</i>	6	$1.70 \pm 0.04$	$6.650 \pm 0.010$	$0.560 \pm 0.000$	$25.96 \pm 1.11$	–0.10																																																																																																																																																	
			<i>R</i>	6	$1.60 \pm 0.04$																																																																																																																																																					

**Notes.**

<sup>a</sup> From the General Catalog of Photometric Data, or the *Hipparcos* Catalog. In either case, these measures are on the Johnson system (Johnson 1965).

<sup>b</sup> From the *Hipparcos* Catalog (ESA 1997).

<sup>c</sup> One of us (B.J.B.) analyzed the spectrum in the ELODIE archive (Moultaka et al. 2004) and obtained this metallicity.

<sup>d</sup> From the ELODIE Catalog (Prugniel & Soubiran 2001).

<sup>e</sup> From the Catalog of Cayrel de Strobel et al. (2001).

Pickles library were calculated in the Johnson filter set and then compared with the values in Schmidt–Kaler (1982). Since these standard literature values assume a quantum efficiency curve that is independent of wavelength, the quantum efficiency curve was omitted from the calculations of colors in the Johnson filter set. This led to a near one-to-one relationship, as seen in Figure 2. For magnitude calculations in both the RIT and WIYN filter sets it was of course necessary to use the quantum efficiency curve, as our observations were taken using the Kodak CCD.

Upon calculating magnitudes for all the sample spectra in each of the essential filters, color–color plots were created.

To achieve more accurate relations between colors, and to reduce error, magnitude values were also separated based on luminosity class prior to fitting. A least-squares fit was then performed leading to a polynomial function, in most cases of order three or less, for each luminosity class. This means that, based on the position of the system on the H–R diagram, a preliminary assignment of the luminosity class of the components of each binary was made; in the few cases where the final determination was in conflict with the initial choice, the calculations were redone for that system with the final luminosity class determinations of the first calculation.

**Table 2**  
Speckle Magnitude Differences and Additional Input Parameters, WIYN Data

WDS ( $\alpha, \delta$ J2000.0)	Discoverer Designation	HIP	Speckle Data			System Parameters			
			$\lambda/\Delta\lambda$ (nm)	No. Obs.	$\Delta m$ (mag)	$V^a$ (mag)	$B - V^a$ (mag)	Parallax <sup>b</sup> (mas)	[Fe/H]
00495+4404	HDS 109	3857	503/40	3	$2.34 \pm 0.03$	$7.776 \pm 0.031$	$0.594 \pm 0.015$	$14.85 \pm 1.32$	$+0.09$
			550/40	2	$2.07 \pm 0.24$				
			648/41	2	$2.09 \pm 0.02$				
			698/39	2	$1.96 \pm 0.12$				
03496+6318	CAR 1	17891	503/40	2	$0.47 \pm 0.03$	$5.860 \pm 0.020$	$0.187 \pm 0.013$	$14.11 \pm 0.64$	...
			550/40	3	$0.51 \pm 0.03$				
			648/41	2	$0.44 \pm 0.03$				
			698/39	7	$0.53 \pm 0.06$				
			754/44	2	$-0.15 \pm 0.54$				
20375+1436	BU 151AB	101769	550/40	8	$0.97 \pm 0.04$	$3.617 \pm 0.016$	$0.458 \pm 0.019$	$33.49 \pm 0.88$	$-0.05^c$
			551/10	3	$1.05 \pm 0.04$				
			648/41	4	$1.13 \pm 0.04$				
			698/39	6	$1.07 \pm 0.02$				
			701/12	6	$1.07 \pm 0.03$				
			754/44	6	$1.12 \pm 0.01$				
21145+1000	STT 535AB	104858	503/40	2	$0.23 \pm 0.03$	$4.487 \pm 0.008$	$0.495 \pm 0.009$	$54.11 \pm 0.85$	$-0.07$
			550/40	5	$0.14 \pm 0.06$				
			551/10	2	$0.19 \pm 0.05^d$				
			648/41	5	$0.28 \pm 0.03$				
			698/39	4	$0.18 \pm 0.06$				
			701/12	2	$0.01 \pm 0.01$				
			754/44	3	$-0.04 \pm 0.16$				
			503/40	2	$0.41 \pm 0.01$				
550/40	4	$0.57 \pm 0.04$							
648/41	3	$0.29 \pm 0.13$							
23411+4613	MLR 4	116849	503/40	2	$0.10 \pm 0.06$	$7.060 \pm 0.070$	$0.465 \pm 0.025$	$14.37 \pm 0.84$	$-0.05$
			550/40	4	$0.30 \pm 0.20$				
			648/41	4	$0.18 \pm 0.10$				
			698/39	4	$0.17 \pm 0.07$				

**Notes.**

<sup>a</sup> From the General Catalog of Photometric Data, or the *Hipparcos* Catalog. In either case, these measures are on the Johnson system (Johnson 1965).

<sup>b</sup> From the *Hipparcos* Catalog (ESA 1997).

<sup>c</sup> One of us (B.J.B.) analyzed the spectrum in the ELODIE archive (Moultaka et al. 2004) and obtained this metallicity.

<sup>d</sup> The standard error derived from the two identical measures from the speckle data is zero and has been replaced by a typical expected value here.

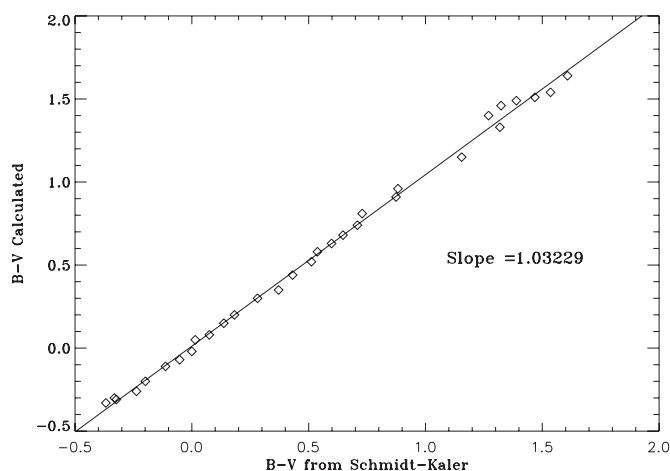


**Figure 2.**  $B - V$  Johnson color magnitudes calculated using the Pickles library and Johnson filter transmission curves, vs. the values found in Schmidt-Kaler. The points were fit with a linear line having a slope of 1.03229, showing our method reproduces the standard color-magnitude values with a small uncertainty.

This then always yielded consistent results in these cases. Also, the Pickles library consists of spectra of single stars, not binaries.

By constructing binary spectra of known input magnitude and color difference between the components, we were able to verify that the color-color relations derived based on single stars do not produce errors of more than a few hundredths of a magnitude when used on synthetic binary systems. Since this is in most cases lower than the uncertainties in our input magnitude differences, this source of error can be ignored at this point. However, in the future, when magnitude differences measures are more numerous and the average result in each filter has greater precision, it may be necessary to devise an iterative scheme for ensuring that magnitude and color calibrations do not dominate the errors in the final results.

System colors in the instrumental filter set were used, along with the speckle magnitude differences, to determine magnitudes for the individual stars in all instrumental filters. This is done using the magnitude difference formula

$$m_b - m_a = 2.5 \log \frac{f_a}{f_b} = \Delta m, \quad (2)$$

where  $m_a$  and  $m_b$  are the magnitudes of the primary and secondary, respectively, and  $f_a$  and  $f_b$  are the fluxes for the primary and secondary, respectively. We can then write the same expression for the binary system as a whole and for a zero-magnitude star. Individual magnitudes for the primary and



secondary can then be found, through simple calculation. Once all the individual magnitudes have been calculated, colors for the primary and secondary can be trivially derived. Finally, with instrumental parameters in hand for each component of the binary, the  $V$  magnitude and  $B - V$  color are obtained with the appropriate inverse transformations, obtained again from the Pickles spectral library.

### 2.2. Isochrone Fitting

Isochrone models were created using  $Y^2$  isochrones and the interpolator program from Yale University (Yi et al. 2001, 2003; Kim et al. 2002; Demarque et al. 2004). Solar metallicity isochrones were generally used since, when known, the iron abundance is usually no more than  $\sim 0.1$  dex away from solar, and the  $[\text{Fe}/\text{H}]$  determinations are probably uncertain on nearly that same level in most cases. In the cases of three stars, we did elect to interpolate the  $Y^2$  isochrones to the metallicity matching the measured iron abundance. These are BU 1163 and COU 2674, which are significantly metal poor, and STF 2912 which is significantly metal rich. Once the metallicity to be used was decided, we created 1800 isochrones for ages of 0.1 to 1.0 Gyr in steps of 0.001 Gyr, and for 1.0 to 9.99 Gyr in steps of 0.01 Gyr. The smaller increments in the younger isochrones were used to provide more precise results for younger systems.

To determine the best fitting, along with upper and lower limit isochrones, we compared our 1800 isochrone models against the primary and secondary positions for a given system. For the purposes of this study, we will refer to the  $1\sigma$  errors associated with the primary and secondary positions as producing an error “rectangle” in the H–R diagram. The isochrones were first linearly upsampled, by a factor of 100, to fill in any spaces between points, as the models can have large gaps between points in areas where the isochrones are relatively straight, i.e., on the main sequence. Next, the isochrones were checked for points falling within the error rectangles. For isochrones which had points lying within the error rectangles, the shortest overall distance of the primary and secondary to the isochrones were determined. The best-fitting isochrone is simply the one which had the shortest overall distance. The age range for a system was simply determined by finding the youngest and oldest isochrones which passed through both error rectangles.

The best-fitting isochrone was then used to estimate the mass range for both the primary and secondary, by determining the portion of the isochrone which falls within the corresponding  $1\sigma$  error. From this we estimate the average mass for both primary and secondary, which are only based on the best-fitting isochrone, and combined them to obtain a total mass for the system. We can then compare this against the total dynamical mass from orbital information. The mass fraction,

$$B = \frac{M_B}{M_A + M_B}, \quad (3)$$

is also calculated, again using only the best-fitting isochrone, from the average mass of the primary,  $M_A$ , and secondary,  $M_B$ .

## 3. RESULTS

### 3.1. CTIO Data

Table 3 contains the derived absolute  $V$  magnitudes and  $B - V$  color magnitudes, in the Johnson filter set, for the components of each system observed at CTIO. Specifically, the columns here give (1) the Discoverer Designation and (2) the *Hipparcos*

Catalog number; (3) the best-fit isochrone age; (4) the age range determined as discussed above; (5) the component identifier for subsequent columns in the table, either A or B; (6) the derived  $B - V$  color and (7) absolute  $V$  magnitude determination; (8) the luminosity class determination; and (9) the mass derived for the component.

Results were derived for all the systems using speckle  $\Delta V$  and  $\Delta R$  magnitudes. For the systems STF 186 (HIP 8998), JC 8AB (HIP 14913), and AC 4 (HIP 32677), a second result was determined using speckle  $\Delta B$  and  $\Delta V$  magnitudes. In these cases, observations were not combined to produce a single result in order to examine any differences which arise from observations in the  $B$  and  $R$  filters, which will be discussed below. While the  $B - V$  color values of the components of these systems are generally different by the order of a tenth of a magnitude, the uncertainties are also typically of the same order. This can be traced back to the uncertainty in individual speckle magnitude differences at the small aperture, as well as the number of observations,  $\leq 8$  in every case. Nonetheless, it can be seen in the final columns of Table 3 that the mass values still have very good precision. This is due to the fact that the color of a component gives leverage mainly on the age of the system, whereas the absolute magnitudes derived affect the mass more than the age in the isochrone fitting. The uncertainties in absolute magnitude depend also on distance, but in general translate into modest uncertainties in the masses of the components.

Systems and components were then separately plotted on the H–R diagrams seen in Figure 3. The solid line is the isochrone which best fits the primary and secondary locations, while the dashed lines represents the isochrones that are the upper and lower age limits. Lines marking the zero age main sequence, subgiant sequence, and giant sequence are also drawn.

For those systems having two sets of results, the H–R diagrams appear in Figure 4. Differences between using  $\Delta B$  and  $\Delta R$  become obvious when comparing these plots. From our results, it is generally the case that the secondary has a redder position in the H–R diagram when the analysis uses the  $B$  and  $V$  filters as opposed to the  $V$  and  $R$  filters. Assuming that the components of a system formed at the same time, the results of the  $R$  observations would appear to be more realistic. This is particularly noticeable in STF 186 (HIP 8998) and JC 8AB (HIP 14913), which have system locations near the main sequence, and where the components would be expected to have positions more or less on the main sequence, especially for the secondary. One possible explanation for this is that the isoplanatic patch is expected to be smaller as the wavelength of observation decreases, thus affecting the  $B$  filter the most. As discussed in Horch et al. (2001), any decorrelation between primary and secondary speckle patterns would lead to an overestimate of the derived magnitude difference. If this effect is most noticeable in the  $B$  filter, a redder color could be derived for the secondary star. Since there are only three systems which had sufficient observations in both  $B$  and  $R$  filters, we cannot draw any definitive conclusions about this; however, the results we have indicate observations taken in the  $R$  filter produce position locations which are more consistent with evolutionary calculations.

### 3.2. WIYN Data

For the objects observed at CTIO, typically data in only two filters were available. This meant that usually only one color–color transformation was needed in order to complete the analysis described above. In contrast, the WIYN objects have

**Table 3**  
Results for CTIO Data

Discoverer	HIP	Age		Comp.	$B - V$	Mv	Lum.	Mass
		Best Fit	Range					
Designation							Class	
BU 395	2941	9.36	0.100–9.99	A	$0.77 \pm 0.14$	$5.31 \pm 0.08$	V	$0.90 \pm 0.01$
				B	$0.68 \pm 0.19$	$5.55 \pm 0.09$	V	$0.87 \pm 0.01$
BU 1163	6564	3.38	1.55–4.40	A	$0.46 \pm 0.08$	$3.34 \pm 0.10$	V	$1.24 \pm 0.02$
				B	$0.36 \pm 0.10$	$3.53 \pm 0.10$	V	$1.20 \pm 0.02$
HJ 3447 <sup>b</sup>	7463	1.27	0.881–1.56	A	$0.39 \pm 0.10$	$2.10 \pm 0.26$	IV	$1.70 \pm 0.08$
				B	$0.22 \pm 0.17$	$3.15 \pm 0.27$	V	$1.45 \pm 0.03$
STF 186	8998	3.62	1.12–6.73	A	$0.54 \pm 0.07$	$3.61 \pm 0.15$	V	$1.25 \pm 0.04$
				B	$0.55 \pm 0.10$	$4.16 \pm 0.16$	V	$1.13 \pm 0.03$
STF 186 <sup>a</sup>	8998	0.696	0.100–6.04	A	$0.44 \pm 0.14$	$3.61 \pm 0.15$	V	$1.32 \pm 0.03$
				B	$0.76 \pm 0.28$	$4.16 \pm 0.16$	V	$1.19 \pm 0.03$
JC 8 AB	14913	1.62	1.41–1.67	A	$0.53 \pm 0.10$	$3.31 \pm 0.09$	V	$1.34 \pm 0.01$
				B	$0.31 \pm 0.15$	$3.71 \pm 0.10$	V	$1.27 \pm 0.002$
JC 8 AB <sup>a,b</sup>	14913	0.281	0.100–3.11	A	$0.32 \pm 0.18$	$3.31 \pm 0.17$	V	$1.41 \pm 0.05$
				B	$0.63 \pm 0.25$	$3.71 \pm 0.19$	V	$1.31 \pm 0.05$
GLE 1	19917	0.169	0.100–1.07	A	$-0.06 \pm 0.34$	$1.55 \pm 0.20$	V	$2.14 \pm 0.25$
				B	$0.26 \pm 0.44$	$1.98 \pm 0.26$	V	$1.90 \pm 0.23$
STT 98 <sup>b</sup>	23879	1.02	0.204–1.49	A	$0.26 \pm 0.11$	$1.80 \pm 0.34$	IV	$1.82 \pm 0.21$
				B	$0.53 \pm 0.22$	$2.98 \pm 0.35$	V	$1.46 \pm 0.17$
AC 4	32677	0.195	0.100–0.386	A	$-0.10 \pm 0.05$	$-0.76 \pm 0.35$	V	$3.62 \pm 0.40$
				B	$-0.08 \pm 0.18$	$0.95 \pm 0.35$	V	$2.52 \pm 0.36$
AC 4 <sup>a</sup>	32677	0.151	0.100–0.267	A	$-0.13 \pm 0.03$	$-0.76 \pm 0.35$	V	$3.92 \pm 0.46$
				B	$0.06 \pm 0.13$	$0.95 \pm 0.35$	V	$2.54 \pm 0.34$
BU 151AB <sup>b</sup>	101769	1.79	1.07–1.96	A	$0.43 \pm 0.14$	$1.58 \pm 0.12$	III	$1.75 \pm 0.002$
				B	$0.56 \pm 0.25$	$2.79 \pm 0.14$	IV	$1.47 \pm 0.04$
STF 2912	111062	0.598	0.100–0.975	A	$0.32 \pm 0.06$	$2.15 \pm 0.14$	IV	$1.82 \pm 0.05$
				B	$0.60 \pm 0.12$	$3.65 \pm 0.15$	V	$1.36 \pm 0.04$
BU 178	113184	2.35	1.14–2.88	A	$0.93 \pm 0.10$	$1.20 \pm 0.19$	III	$1.62 \pm 0.00$
				B	$0.58 \pm 0.19$	$2.96 \pm 0.20$	V	$1.42 \pm 0.05$
SEE 492	116436	3.42	0.100–6.14	A	$0.54 \pm 0.05$	$3.97 \pm 0.09$	V	$1.17 \pm 0.02$
				B	$0.70 \pm 0.09$	$5.66 \pm 0.10$	V	$0.91 \pm 0.01$

**Notes.**

<sup>a</sup> Calculated using  $\Delta B$  and a system  $B - V$  color magnitude.

<sup>b</sup> The best-fit isochrone does not simultaneously run through the  $1\sigma$  error bar for the primary and secondary (but does simultaneously fit the  $2\sigma$  error bars).

been observed in at least three, and up to seven, filters. This presents additional work in completing the analysis, though essentially the same method described above was simply used multiple times. For every filter pair that could reasonably be used to generate a color, color–color transformations were created from the Pickles spectral library, and estimates of the component  $M_V$  and  $B - V$  values were obtained. Once all possible estimates were obtained, average values were formed.

In Table 4, we show the results for the component  $V$  magnitudes and  $B - V$  colors as well as the results from the isochrone fitting for objects observed at the WIYN Telescope. The column headings are exactly the same as in Table 3. In this case, it is possible to see the advantage of the larger aperture, particularly on the derived  $B - V$  values for the components. Values for the component masses are likewise relatively precise, with estimated uncertainties under 0.1 solar masses for the primaries in all cases. The H–R diagrams for these systems are shown in Figure 5.

#### 4. DISCUSSION

Upon surveying the results in Tables 3 and 4, we can first conclude that in most cases the age information is only rudimentary; as most systems are on or near the main sequence, no precise ages can be determined. In a few cases, however, one or both components is evolved. The best example of this

is BU 151AB, where from CTIO data the age range matching the H–R diagram positions is 1.07 to 1.96 Gyr with a best-fit value of 1.79 Gyr, and for WIYN data on the same system, it is 1.60 to 1.94 Gyr with a best-fit value of 1.76 Gyr. The excellent agreement between the data sets gives confidence that the photometric conversions are working well. This system is discussed further below.

Tables 5 and 6 provide a comparison between the masses derived here and those available from orbit determinations and other data in the literature. The column headings for both give (1) *Hipparcos* Catalog number; (2) the mass fraction and (3) total mass calculated from the isochrone fitting, in solar masses; (4) the dynamically determined mass fraction, if it exists, and (5) total mass from orbit calculations; and (6) the reference for the orbit calculation. Dynamically determined mass fractions are those appearing in Meyer (2002). In many cases, the orbital parameters are published without uncertainties, meaning that it is not possible to properly account for the contributions of the uncertainties in the semimajor axis and period in the uncertainty of the dynamical mass sum. This is noted in the relevant cases in Column (5) of these tables. The errors shown in these cases are only those due to the uncertainty in the parallax, and while it is true that in most cases the parallax is almost certainly the dominant source of uncertainty in the mass sum, the values listed are still necessarily an underestimate.

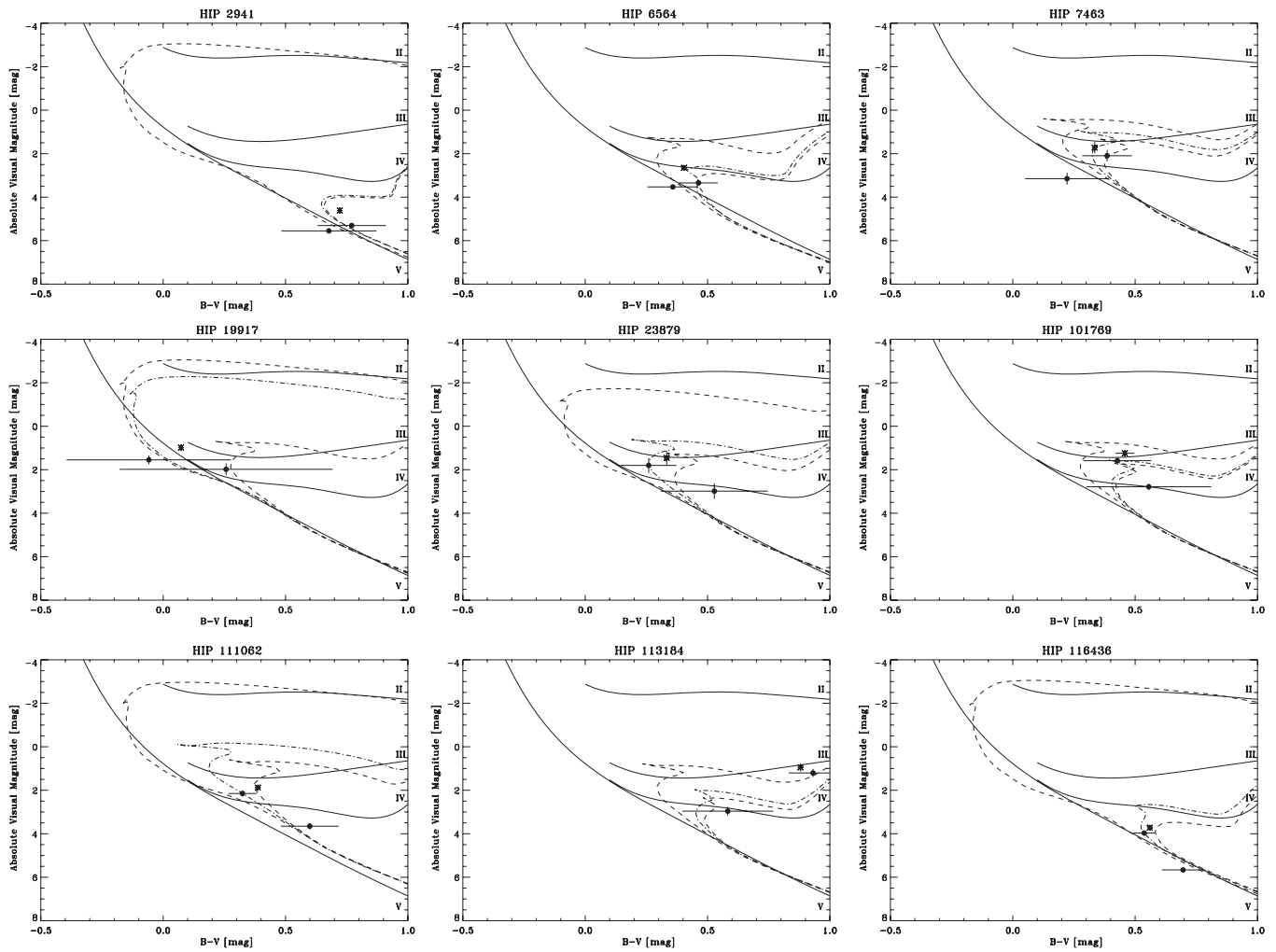


Figure 3. H-R diagrams for the nine CTIO systems in Table 3 having only *V* and *R* measures.

Table 4  
Results for WIYN Data

Discoverer	HIP	Age		Comp.	<i>B</i> − <i>V</i>	<i>M</i> <sub>v</sub>	Lum.	Mass
Designation		Best Fit	Range				Class	
HDS 109	3857	3.87	0.881–5.86	A	0.55 ± 0.03	3.77 ± 0.44	V	1.21 ± 0.09
				B	0.82 ± 0.05	6.01 ± 0.44	V	0.88 ± 0.03
CAR 1	17891	0.302	0.100–0.468	A	0.18 ± 0.02	2.14 ± 0.23	IV	1.76 ± 0.18
				B	0.20 ± 0.03	2.63 ± 0.23	V	1.67 ± 0.17
BU 151 AB	101769	1.76	1.60–1.94	A	0.49 ± 0.02	1.60 ± 0.13	III	1.760 ± 0.001
				B	0.40 ± 0.04	2.63 ± 0.13	IV	1.52 ± 0.04
STT 535	104858	2.34	0.76–3.36	A	0.50 ± 0.02	3.81 ± 0.08	V	1.22 ± 0.02
				B	0.52 ± 0.04	4.01 ± 0.08	V	1.18 ± 0.02
COU 2674	116578	7.61	0.100–9.99	A	0.45 ± 0.06	4.16 ± 0.73	V	0.92 ± 0.07
				B	0.57 ± 0.08	4.52 ± 0.73	V	0.86 ± 0.04
MLR 4	116849	2.02	0.100–2.57	A	0.48 ± 0.03	3.51 ± 0.29	V	1.27 ± 0.04
				B	0.43 ± 0.05	3.65 ± 0.29	V	1.29 ± 0.03

Comparing the mass sums determined photometrically with those determined dynamically, the overall agreement is excellent. The three exceptions to this are for STT 98, BU 178, and SEE 492, which are all discussed in the following subsection. To gauge the degree to which our results depend on the  $Y^2$  isochrones, we have compared the result using the  $Y^2$  isochrones in some cases with the Padova isochrones of Girardi et al. (2000), also available online.<sup>13</sup> Figure 6 shows the result of

a typical comparison. In general, we have found little difference between the two sets of isochrones, which is to be expected since many of our systems are main-sequence or just-evolved systems.

We have also explored the effect of choosing a different metallicity for the isochrone set. This is important especially since some of our systems do not have abundance determinations. We find that the masses derived increase by two to three percent when using metal-rich isochrones with iron abundance +0.34, and decrease approximately seven percent when using

<sup>13</sup> <http://pleiadi.pd.astro.it>

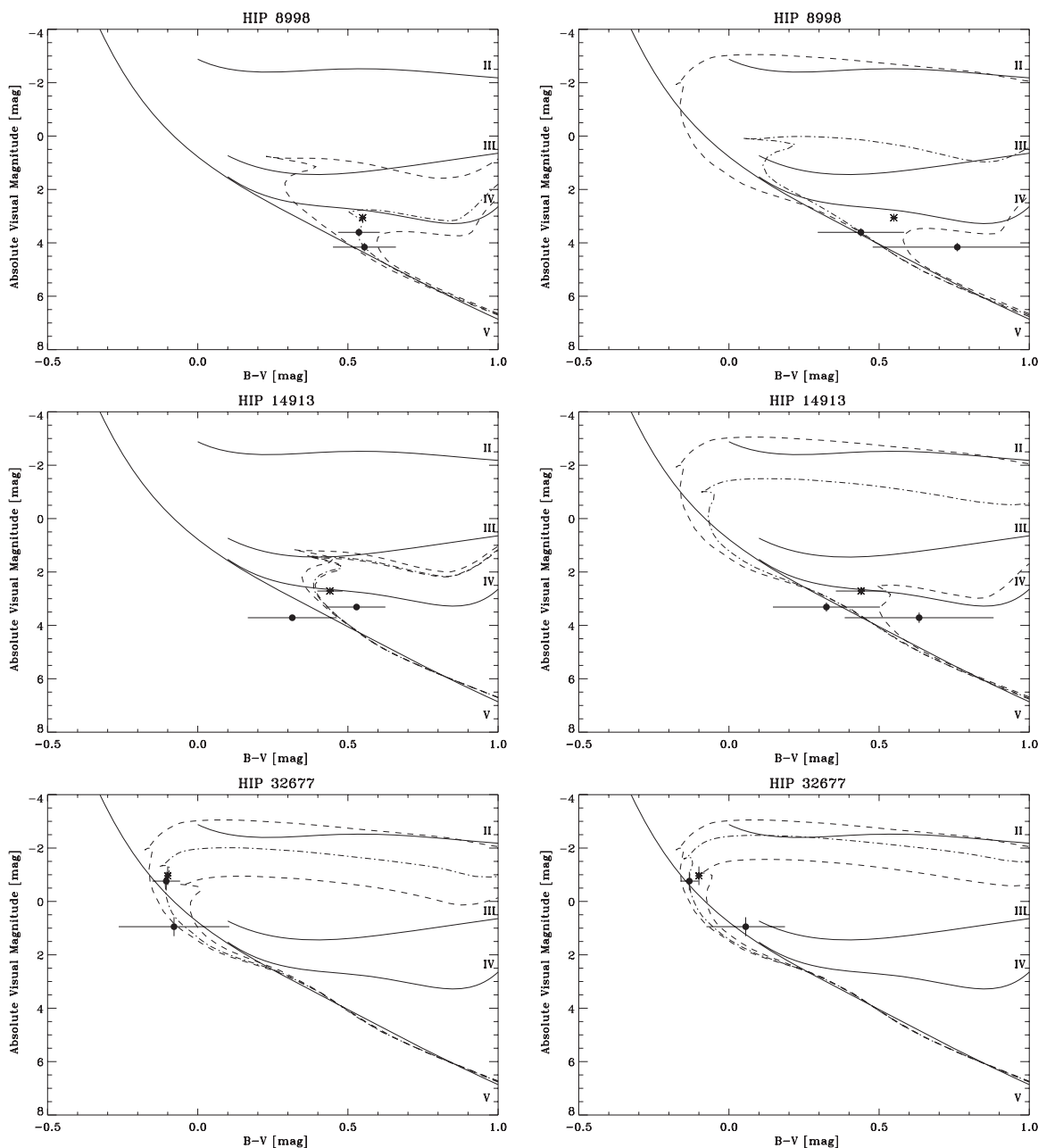


Figure 4. H–R diagrams for three CTIO systems using both  $V - R$  (left) and  $B - V$  (right) speckle magnitude differences.

metal-poor isochrones with iron abundance  $-0.25$ . This indicates that certainly systems with metal abundance in the range  $-0.15$  to  $+0.15$  would suffer only a minor correction from what is derived here using solar values, one which is not significant given our uncertainties at this stage. To be conservative, we have added a 10% uncertainty in quadrature with the uncertainties obtained from the isochrone fitting to mass values to systems for which no iron abundance is available.

#### 4.1. Notes on Specific Systems

Several systems in the data set deserve special mention.

1. **BU 395** (HIP 2941). Due to the calculation of Pourbaix (2000), we have a very good orbit, listed as Grade 1 in the Sixth Orbit Catalog<sup>14</sup> (Hartkopf et al. 2001) and a mass

uncertainty of only  $\sim 0.1 M_{\odot}$ . Of the systems observed at CTIO, this is the smallest dynamical mass uncertainty. Our total mass value matches that derived from the Pourbaix orbit almost exactly, although there is a discrepancy in the mass fraction. This will have to be monitored and reevaluated in the coming years as more data become available.

2. **STT 98** (HIP 23879). The dynamical mass sum of this object is  $5.45 M_{\odot}$  (with an uncertainty of well over  $1 M_{\odot}$ , considering that the orbital parameters were published without uncertainties), and the  $B - V$  color for the system is 0.334. Given that the components appear to be near the main sequence (with the primary slightly evolved) and that the system has a modest magnitude difference of approximately 1 mag, one would expect spectral types of perhaps F0 and F5. Using data in Schmidt–Kaler, this would yield masses of approximately 1.6 and 1.4 solar masses, that is, a mass

<sup>14</sup> <http://ad.usno.navy.mil/wds/orb6.html>



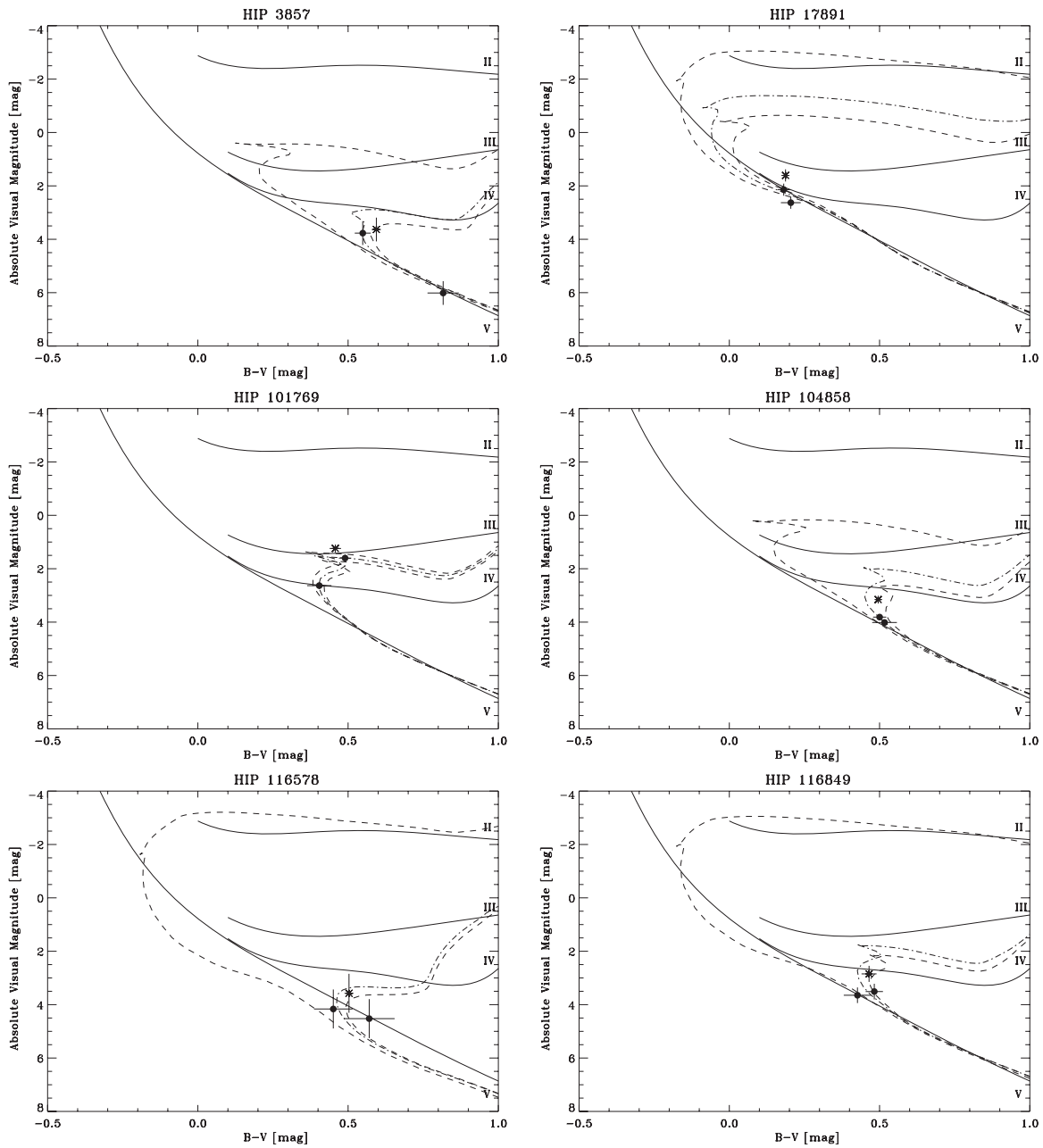


Figure 5. H-R diagrams for the six WIYN systems in Table 4.

sum of approximately 3 solar masses. The orbit is given a grade of 2 in the Sixth Orbit Catalog, but the period is 197 years, so that modern astrometric techniques do not cover the majority of the orbit. We suggest that the mass sum deduced from this orbit may be an overestimate. In our previous work (Horch et al. 2001), we derived preliminary colors and temperatures of the components; the work here is consistent with those earlier results.

3. **BU 151AB** (HIP 101769). As mentioned above, this system consists of two evolved stars, allowing for a relatively precise age determination from both CTIO and WIYN data. The orbit of Alzner (1998) is of excellent quality, easily grade 1 in the Sixth Orbit Catalog, and was produced from high-quality speckle data spanning over a full orbit. This represents one of the most interesting tests of our method, since the uncertainty in the dynamical mass sum is only about three tenths of a solar mass, and the components are

evolved. The agreement between the dynamical value and those of both the CTIO and WIYN results is nearly perfect.

4. **STT 535AB** (HIP 104858). This main-sequence system has a very precise orbit determination, published with uncertainties. The uncertainty in the mass sum is only a tenth of a solar mass, making this object the best pure test of our photometrically derived mass values for WIYN data. Our value is well within  $1\sigma$  of the dynamical value. Our mass fraction also agrees, though we still have an uncertainty of over 10% in this number at present.
5. **BU178** (HIP 113184). This system has the largest discrepancy between the dynamical mass sum and that derived from the photometric analysis presented here. We find the primary to be a giant, which is consistent with the red system  $B - V$  color of  $\sim 0.9$ , with the secondary still on or near the main sequence. The orbit has a period of 97 years, and the dynamical mass sum is  $8.67 \pm 2.22 M_{\odot}$ , with the

**Table 5**  
CTIO Mass Results Compared with Literature Values

HIP	Photometric Results		Dynamical Results		Orbit Reference
	Mass Fraction	Total Mass	Mass Fraction	Mass Sum	
2941	0.49 ± 0.01	1.76 ± 0.01	0.42 ± 0.02	1.77 ± 0.13	Pourbaix (2000)
6564	0.49 ± 0.01	2.44 ± 0.03	0.52 ± 0.03	2.73 ± 0.34 <sup>a</sup>	Söderhjelm (1999)
7463	0.46 ± 0.01	3.15 ± 0.09	...	3.19 ± 0.72	Cvetković & Novaković (2006)
8998 (V,R)	0.48 ± 0.02	2.38 ± 0.05	<sup>b</sup>	2.05 ± 0.41 <sup>a</sup>	Brendley & Mason (2007)
8998 (B,V)	0.48 ± 0.02	2.51 ± 0.05	"	"	"
14913 (V,R)	0.49 ± 0.002	2.61 ± 0.01	0.51 ± 0.05	2.84 ± 0.29 <sup>a</sup>	Söderhjelm (1999)
14913 (B,V)	0.48 ± 0.02	2.72 ± 0.06	"	"	"
19917	0.47 ± 0.07	4.05 ± 0.34	...	5.14 ± 0.97 <sup>a</sup>	Docobo & Ling (2006)
23879	0.45 ± 0.07	3.28 ± 0.28	...	5.45 ± 1.28 <sup>a</sup>	Scardia et al. (2008)
32677 (V,R)	0.41 ± 0.07	6.15 ± 0.54	...	...	...
32677 (B,V)	0.39 ± 0.06	6.46 ± 0.57	"	"	"
101769	0.46 ± 0.01	3.22 ± 0.04	0.45 ± 0.02	3.25 ± 0.26 <sup>a</sup>	Alzner (1998)
111062	0.43 ± 0.01	3.18 ± 0.06	...	3.52 ± 0.69 <sup>a</sup>	Söderhjelm (1999)
113184	0.47 ± 0.02	3.04 ± 0.05	...	8.67 ± 2.22 <sup>a</sup>	Brendley & Mason (2007)
116436	0.44 ± 0.01	2.08 ± 0.02	...	1.67 ± 0.21 <sup>a</sup>	Heintz (1984)

**Notes.**

<sup>a</sup> The actual uncertainty is greater than that listed due to the fact that the orbital elements were published without uncertainties. The value given is solely due to parallax.

<sup>b</sup> A value is reported in Meyer (2002); however, it is aphysical, and has not been included.

**Table 6**  
WIYN Mass Results Compared with Literature Values

HIP	Photometric Results		Dynamical Results		Orbit Reference
	Mass Fraction	Total Mass	Mass Fraction	Mass Sum	
3857	0.42 ± 0.03	2.08 ± 0.10	...	...	...
17891	0.49 ± 0.06	3.43 ± 0.25	...	3.65 ± 0.50 <sup>a</sup>	Zirm & Horch (2002)
101769	0.46 ± 0.01	3.28 ± 0.04	0.45 ± 0.02	3.25 ± 0.26 <sup>a</sup>	Alzner (1998)
104858	0.49 ± 0.01	2.40 ± 0.02	0.484 ± 0.004	2.42 ± 0.11	Muterspaugh et al. (2008)
116578	0.48 ± 0.03	1.78 ± 0.08	...	...	...
116849	0.50 ± 0.02	2.56 ± 0.05	...	2.50 ± 0.44	Hartkopf et al. (1996)

**Note.** <sup>a</sup> The actual uncertainty is greater than that listed due to the fact that the orbital elements were published without uncertainties. The value given is solely due to parallax.

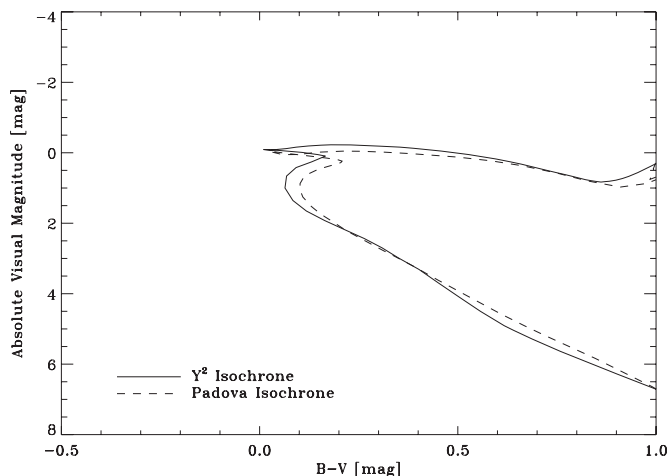


**Figure 6.** Comparison of a  $Y^2$  isochrone with a Padova isochrone, both with Solar metallicity and age of 0.598 Gyr.

uncertainty being an underestimate due to the lack of error estimates for the orbital elements. The orbit leading to this mass sum is given a grade of 4 in the Sixth Orbit Catalog, but interestingly does include one early interferometric observation of Maggini in 1923 quoted in the 4th

Interferometric Catalog. We note that an earlier orbit of Baize (1981), when combined with the *Hipparcos* parallax, gives a mass sum of nearly  $10 M_{\odot}$ , so that at least the accumulation of speckle data since 1981 has decreased the mass somewhat. Nonetheless, we suggest that the dynamical mass value should not be given significant weight at this time.

6. **SEE 492** (HIP 116436). In this case there is a nearly  $2\sigma$  discrepancy between the mass sum obtained here and that deduced from the dynamical information. Again, the orbit is listed as grade 4 in the Sixth Orbit Catalog, with a period of 78.5 years. We also note that the most recent observations appear to deviate from the orbit prediction, suggesting that an orbit revision may be needed in the coming years.

## 5. CONCLUSIONS

Component masses have been estimated for 17 binary star systems using speckle photometry and isochrone fitting. We have shown that our total system masses are consistent with those determined using orbital parameters. Three systems had no prior mass determinations, and the work here has provided component masses for the first time. It has also provided mass fractions in some cases where only a mass sum had previously been determined dynamically. Generally, the results obtained

here are of higher precision than the dynamically determined masses. We suggest that this method has promise in the statistical studies of binaries, where it could provide mass information in a relatively short period of time without recourse to orbital data.

We gratefully acknowledge funding from the National Science Foundation, Grants AST 03-07450 and AST 05-04010, which provided support for two of us (J.W.D. and B.J.B.) while graduate students at UMass Dartmouth. We also thank the American Astronomical Society for two small research grants, which funded the observing trips to CTIO. This work made use of the Washington Double Star Catalog maintained at the U.S. Naval Observatory, the SIMBAD database, operated at CDS, Strasbourg, France, and the NASA/IPAC Infrared Science Archive, which is operated by the Jet Propulsion Laboratory, California Institute of Technology, under contract with the National Aeronautics and Space Administration.

## REFERENCES

- Alzner, A. 1998, *A&AS*, **132**, 253  
 Baize, P. 1981, *A&AS*, **44**, 199  
 Bessel, M. S. 1990, *PASP*, **102**, 1181  
 Brendley, M., & Mason, B. D. 2007, *IAU Comm. 26 Inf. Circ.* 163  
 Cayrel de Strobel, G., Soubiran, C., & Ralite, N. 2001, *A&A*, **373**, 159  
 Cvetković, Z., & Novaković, B. 2006, *Serbian AJ*, **173**, 73  
 Demarque, P., Woo, J.-H., Kim, Y.-C., & Yi, S. K. 2004, *ApJS*, **155**, 667  
 Docobo, J. A., & Ling, J. F. 2006, *IAU Comm. 24 Inf. Circ.* 158  
 ESA. 1997, in *The Hipparcos and Tycho Catalogues* (ESA SP-1200) (Noordwijk: ESA)  
 Fernie, J. D. 1983, *PASP*, **95**, 782  
 Girardi, L., Bressan, A., Bertelli, G., & Chiosi, C. 2000, *A&AS*, **141**, 371  
 Hartkopf, W. I., Mason, B. D., & McAlister, H. A. 1996, *AJ*, **111**, 370  
 Hartkopf, W. I., Mason, B. D., & Worley, C. E. 2001, *AJ*, **122**, 3472  
 Heintz, W. D. 1984, *AJ*, **89**, 1063  
 Horch, E. P., Baptista, B. J., Veillette, D. R., & Franz, O. G. 2006a, *AJ*, **131**, 3008  
 Horch, E. P., Davidson, J. W., van Altena, W. F., Girard, T. M., Lopez, C. E., Franz, O. G., & Timothy, J. G. 2006b, *AJ*, **131**, 1000  
 Horch, E. P., Dinescu, D. I., van Altena, W. F., Girard, T. M., Lopez, C. E., & Franz, O. G. 1996, *AJ*, **111**, 1681  
 Horch, E. P., Meyer, R. D., & van Altena, W. F. 2004, *AJ*, **127**, 1727  
 Horch, E. P., Ninkov, Z., & Franz, O. G. 2001, *AJ*, **121**, 1583  
 Horch, E. P., Ninkov, Z., van Altena, W. F., Meyer, R. D., Girard, T. M., & Timothy, J. G. 1999, *AJ*, **117**, 548  
 Horch, E. P., van Altena, W. F., Cyr, W. M., Kinsman-Smith, L., Srivastava, A., & Zhou, J. 2008, *AJ*, **136**, 312  
 Johnson, H. L. 1965, *ApJ*, **141**, 923  
 Kim, Y.-C., Demarque, P., Yi, S. K., & Alexander, D. R. 2002, *ApJS*, **143**, 499  
 Mason, B. D., Hartkopf, W. I., Wycoff, G. L., & Wieder, G. 2007, *AJ*, **134**, 1671  
 Mason, B. D., Wycoff, G. L., Hartkopf, W. I., Douglass, G. G., & Worley, C. E. 2001, *AJ*, **122**, 3466  
 Mermilliod, J. C., Mermilliod, M., & Hauck, B. 1997, *A&AS*, **124**, 349  
 Meyer, R. D. 2002, PhD thesis, Yale Univ.  
 Meyer, R. D., Horch, E. P., Ninkov, Z., van Altena, W. F., & Rothkopf, C. A. 2006, *PASP*, **118**, 162  
 Moultaqa, J., Ilovaisky, S. A., Prugniel, P., & Soubiran, C. 2004, *PASP*, **116**, 693  
 Muterspaugh, M. W., et al. 2008, *AJ*, **135**, 766  
 Nordström, B., et al. 2004, *A&A*, **418**, 989  
 Pickles, A. J. 1998, *PASP*, **110**, 863  
 Pourbaix, D. 2000, *A&AS*, **145**, 215  
 Prugniel, P., & Soubiran, C. 2001, *A&A*, **369**, 1048  
 Samus', N. N., Durlevich, O. V., Zharova, A. V., Kazarovets, E. V., Kireeva, N. N., Pastukhova, E. N., Williams, D. B., & Hazen, M. L. 2006, *Astron. Lett.*, **32**, 263  
 Scardia, M., Prieur, J.-L., Pansecchi, L., & Argyle, R. W. 2008, *IAU Comm. 24 Inf. Circ.* 164  
 Schmidt-Kaler, T. 1982, in *Landolt-Börnstein New Series, Group 6, Vol. 2b, Stars and Star Clusters*, ed. K. Schaifers & H.-H. Voigt (Berlin: Springer), 17  
 Söderhjelm, S. 1999, *A&A*, **341**, 121  
 Yi, S., Demarque, P., Kim, Y.-C., Lee, Y.-W., Ree, C. H., Lejeune, T., & Barnes, S. 2001, *ApJS*, **136**, 417  
 Yi, S. K., Kim, Y.-C., & Demarque, P. 2003, *ApJS*, **144**, 259  
 Zirm, H., & Horch, E. P. 2002, *IAU Comm. 24 Inf. Circ.* 147